Available online at www.sciencedirect.com
SCIENCE DIRECT®
Polymer 44 (2003) 4411–4420
polymer
www.elsevier.com/locate/polymer

Characterization of electrosterically stabilized polystyrene latex; implications for radical entry kinetics

Hank De Bruyn[a], Robert G. Gilbert[a,*], John W. White[b], Jamie C. Schulz[c]

[a]*Key Centre for Polymer Colloids, School of Chemistry F11, University of Sydney, NSW 2006, Australia*
[b]*Research School of Chemistry, Australian National University, Canberra, ACT 0200, Australia*
[c]*Center for Neutron Research*[1]*, National Institute of Standards and Technology, Gaithersburg, MD, USA*

Received 26 March 2003; received in revised form 1 June 2003; accepted 3 June 2003

Abstract

Electrosterically stabilized polystyrene latexes with a poly(acrylic acid) hydrophilic layer with either perdeuterated core or perdeuterated hydrophilic layer were prepared in situ in a styrene/acrylic acid copolymerization, in a manner similar to that commonly employed industrially. Small angle neutron scattering (SANS) measurements were made over a range of contrasts for three latexes at high and low pH. Parameters obtained by fitting to standard core/shell models were consistent with the shell being highly hydrated (about 89% at low pH and about 94% at high pH). The core was found to contain about 3% acrylic acid. Doubling the proportion of acrylic acid in the recipe increased shell thickness by about 20%, slightly reduced particle size and slightly increased the proportion of acrylic acid incorporated into the core. The maximum degree of polymerization (DOP) of the entering (and therefore grafted) species was estimated from the shell thickness to be about 44 monomer units for 0.02 M acrylic acid and 66 for 0.04 M. The observed dependence of hairy layer (shell) thickness on the initial amount of acrylic acid suggests that the critical DOP for entry (and therefore true grafting) of the electrosteric stabilizer is thermodynamically (not kinetically) controlled.

Keywords: Latex; SANS; Styrene

1. Introduction

The general understanding of the mechanisms, rate coefficients and outcomes of emulsion polymerizations with relatively hydrophobic monomers (e.g. styrene and MMA) is at a moderately advanced level [1] but one area where significant understanding is needed is for systems containing hydrophilic monomers. The use of hydrophilic monomers (as co-monomers in conjunction with hydrophobic monomers) is common in industrial emulsion polymerizations [2]. A generic industrial surface-coating 'recipe' might comprise methyl methacrylate and butyl acrylate as hydrophobic monomers, a few percent of acrylic acid (AA) as the hydrophilic co-monomer [3] plus varying types of steric and/or electrostatic stabilizer(s). The resulting colloids are electrosterically stabilized with good colloidal stability and desirable film-forming properties. However, there is little fundamental scientific understanding of the effects of hydrophilic monomers on the polymerization process and products. This is not surprising: even in the absence of the hydrophobic monomers, the aqueous-phase polymerization of hydrophilic monomers is extremely complex (e.g. [4–6]). However, hydrophilic monomers have profound effects: for example, we have shown [7] that models which have been successful in predicting the rate coefficients for free-radical entry and exit, and particle formation, in emulsion polymerization of hydrophobic monomers fail for latexes heavily coated with electrosteric stabilizers (the 'hairy layer') containing a hydrophilic monomer (acrylic acid).

In emulsion polymerizations in Interval II (in the absence of particle formation), it is well established [8–12] that for electrostatically stablized latexes, the entry mechanism is

* Corresponding author. Tel.: +61-2-9351-3366; fax: +61-2-9351-8651.
E-mail address: gilbert@chem.usyd.edu.au (R.G. Gilbert).

[1] Certain trade names and company products are identified to adequately specify the experimental procedure. In no case does such identification imply recommendation or endorsement by the National Institute of Standards and Technology, nor does it imply that the products are necessarily the best for the purpose.

0032-3861/03/$ - see front matter © 2003 Elsevier Science Ltd. All rights reserved.
doi:10.1016/S0032-3861(03)00452-X

aqueous-phase propagation of an oligomeric radical derived from initiator until a degree of polymerization (DOP) z is achieved, so that the resulting species (e.g. $(styrene)_3SO_4^-$ in the case of styrene with persulfate initiator) becomes surface-active and irreversibly enters a particle; entry is only through these z-mers (and any larger species). The entry rate of a z-mer in electrostatically stabilized systems has been found to be proportional to particle radius [13], strongly suggesting that this process is diffusion controlled; the actual entry of a z-mer is supposed to be so fast as not to be rate-determining in electrostatically stabilized systems. For exit, it is well established [1,14] that the mechanism is transfer to monomer to form an oligomeric radical which can rapidly diffuse through the particle and into the water phase, with diffusion away from the particle being one of the rate-determining steps. However, in systems with a heavy coating of an electrosteric stabilizer, it has been found [7] that there is a significant reduction in both the entry and exit rate coefficients. This is consistent with movement of both an entering z-mer and an exiting monomeric radical through the hairy layer being slowed down by diffusion through this viscous region. Moreover, these diffusive events are rate-determining in particle formation [1]. Hence, it is important for qualitative and quantitative understanding of entry, exit and nucleation that there are means to characterize this hairy layer: (i) its spatial extent, (ii) the distribution of hydrophilic monomer units as a function of distance from the particle surface, and (iii) diffusion coefficients of small species within this hairy layer. This paper establishes the methodology to determine the first of these, and to obtain semi-quantitative information about the second.

The main objective of this work was to determine the thickness and density (and the pH dependence of these properties) of a poly(acrylic acid) shell on polystyrene latexes. To the best of our knowledge, this is the first time the internal structure of an in situ hairy layer has been measured directly in a system which is representative of that used to provide freeze-thaw colloidal stability in an industrial surface coating.

Previous studies have shown that the effects of hydrophilic monomers are complex, even when attempts are made to vary only a single parameter at a time. Even with the best of these studies (e.g. [15]), there have been no unambiguous mechanistic conclusions, because if, for example, one changes the amount of a hydrophilic monomer in a recipe, then particle size and particle number will change, as well as entry and exit rate coefficients.

Techniques employed to study hairy layers include sedimentation [2], photon correlation spectroscopy (PCS) [16], dynamic light-scattering (DLS) [17] and conductometric titrations [7,18,19].

Bassett and Hoy were the pioneers in this field. Their sedimentation studies on electrosterically stabilized acrylate latexes [2] showed that the expansion of the hairy layer is very sensitive to high pH, increasing dramatically from 8 to 10, then decreasing almost as rapidly from pH = 10 to 12. The decrease at high pH is probably due to the concomitant increase in electrolyte concentration (they also showed that expansion is approximately halved at 0.01 M NaCl and halved again at 0.1 M NaCl). They found maximum expansions of 50–120 nm. When the same methodology was applied to a styrene/AA latex no expansion was observed and at high pH the apparent shell thickness actually decreased by about 7 nm. This surprising result was accredited to backbone stiffness; however, in light of the work presented herein it seems more likely that the hairy layer in the styrene/AA system is too small and/or hydrated to be measured accurately by the sedimentation technique employed. Another limitation of sedimentation is that it yields little information regarding internal structure.

The same can be said for light-scattering techniques, although one interesting exception is the work of Guo et al. [17]. These authors grew a hairy poly(acrylic acid) (pAA) layer on polystyrene latexes coated with a photoinitiating ester. After characterizing the hairy layer by DLS (diameter as function of [AA] and [electrolyte]), they hydrolyzed the ester and characterized the pAA chains independently. They found typical hairy layer thickness of about 60 nm and average MW of 56,400 with each 'hair' occupying a surface area on the particle of $\sim$43 nm^2. This gives an inter-grafting site distance of about 7 nm. A pAA chain of this MW should have a hydrodynamic radius greater than 15 nm under their experimental conditions so clearly the chains are being 'squeezed' onto the particle and thus the shell thickness is several times the hydrodynamic radius of the equivalent MW random coil. This has implications for the interpretation of the shell thickness data acquired in this work (see below). Recent work by Fritz et al. [20] gains additional information by combining light-scattering with viscosity data.

Conductometric titrations reveal the distribution of carboxylic acid groups between the aqueous-phase, particle surface and particle interior but tend to give conflicting results [21]. Small angle neutron scattering (SANS) gives an independent and much more reliable measure of incorporated pAA (see below).

Small-angle X-ray scattering (SAXS) has been used to good effect to characterize core/shell particles [22]. Contrast matching is possible (see below) by dissolving a high electron density substance, such as D-glucose, in the continuous-phase [23]; however, the contrast between a highly swollen hairy layer and the continuous-phase (especially after the continuous-phase has been contrast-matched to the core) is too low to produce useful results. Furthermore, the presence of high concentrations of glucose may affect the characteristics of the hairy layer.

Small-angle neutron scattering (SANS) is the only technique that permits the in situ characterization of the thickness and hydration of a hairy layer grown in situ. In SANS, neutrons penetrate latexes with little loss of intensity (typical sample-cell path length $\sim$1 mm) allowing direct measurement of latex particles in suspension. Thermal

neutron wavelengths are similar to those of X-rays (typically 0.2–1 nm), providing resolution of the order of 0.1 nm. In soft-condensed materials such as polymers, SANS has several advantages.

Contrast variation is a useful SANS tool for inferring the composition of colloidal particles [24]. This approach takes advantage of the distinctive scattering length densities of different atoms (or in the case of SAXS, differences in electron densities), particularly the large difference in scattering length densities (SLDs) of hydrogen and deuterium. In the present work, two contrast variation methods are employed: internal and external contrast variation. Internal contrast variation involves the selective deuteration of a particular component, and in this study perdeuterated styrene and perdeuterated acrylic acid were used to produce latexes with either a perdeuterated core or a perdeuterated hairy layer. In external contrast variation, the scattering length density of the solvent is varied by using mixtures of D_2O and H_2O.

This versatility is employed in a well-established technique called 'contrast matching' wherein the solvent SLD is adjusted to match one of the components of the system to be studied. That component is then said to be 'matched out' and scatters like solvent. Consequently, those components, which may be present at low concentrations, or simply scatter weakly, may be more readily measured. This is crucial in this work as the object of our inquiry, the hairy layer, suffers from both these deficiencies—it represents only about 5% of the total polymer incorporated into the latex (i.e. only about 0.05% of sample mass) and, as it is likely to be highly hydrated, the contrast between hairy layer and the continuous-phase is minimal; hence it scatters weakly.

2. Materials and methods

The first consideration in this work was to produce electrosterically stabilized latexes representative of those used in typical industry preparations, i.e. with a shell of pAA grown in situ by copolymerizing AA with styrene. The second consideration was that for reliable quantitative fitting of SANS data, it is essential to minimize polydispersity. Thirdly, it was desirable to use as little deuterated monomer as possible. The following recipes satisfied all these criteria.

Deuterated stock latexes were prepared using the quantities detailed in Table 1. AMA-80 (sodium dihexyl sulfosuccinate and a few branched isomers thereof, Cyanamid), acrylic acid (Sumika Glacial Acrylic Pte Ltd) or perdeuterated acrylic acid (Aldrich), styrene (Aldrich) or perdeuterated styrene (Aldrich, 98%+) (all used as received) were added to thoroughly deoxygenated water, flooded with high purity argon (BOC Gases) and sealed in 250 ml glass flasks (equipped with crown seals and septa). The flasks were then placed in a bath at 90°C and tumbled at 45 rpm for 30 min, whereafter a solution of recrystallized potassium persulfate (Merck) was injected. The reaction was maintained at 90°C for two hours (final pH 2.7). The latexes were dialyzed for three days with six changes of water then centrifuged and resuspended three times (2 h at 20,000 rpm then 2 h at 40,000 rpm twice) with the final resuspension being in D_2O (Aldrich 99.9%D) (for latexes A and B) and H_2O for latex C (perdeuterated acrylic acid 'hairy layer'). The centrifugate was a 'gel pellet' which contained about 50% H_2O; this must be taken into account when calculating SLDs of the aqueous-phase (latex A: 46%, B: 51%). The final pH was 6.4 for stock latexes A and C, pH 5.6 for B. MilliQ water, 18.2 MΩ cm^{-1} was used throughout. A typical micrograph of the latexes so produced is shown in Fig. 1.

It is expected that the particles will have a smooth surface, because the synthesis was performed at 90 °C, only 10 °C below its glass transition temperature, and hence the particles will be above the glass transition temperature of the monomer-swollen polymer during virtually all of the batch synthesis process.

2.1. Critical coagulation concentration experiments

The pH dependence of the stability conferred on latexes by the hairy layer was determined by turbidimetry according to the method of Overbeek [25]. The turbidity of the latexes, after removal of surfactant by dialysis and centrifugation, was measured in a spectrophotometer cell (680 nm) as a function of time and [KCl] at low and high pH. (Fig. 2). The stability ratio, W, is defined as the initial slope of the turbidity vs time curve at high [KCl] over the initial slope at a given [KCl]. A log–log plot of W vs [KCl] then gives the critical coagulation concentration (CCC) as the [KCl] above which $W = 1$ (Fig. 3). It can be seen in Fig. 2 that at high pH the electrosterically stabilized polystyrene latex is extremely stable to electrolyte. At pH 2 the same latex had a slightly lower CCC (0.6 M KCl) than an anionically

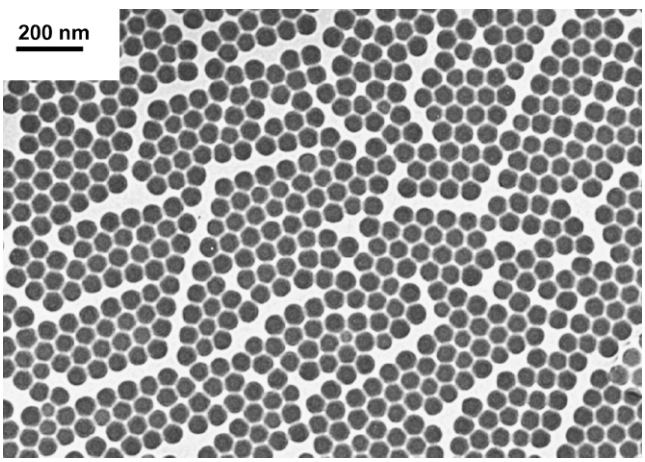

Fig. 1. TEM micrograph of latex A (deuterated core). Note hexagonal packing-indicative of low polydispersity.

Table 1
Latex recipes. Molarities based on water content of latexes

	Latex A		Latex B		Latex C		Undeuterated	
	g	M	g	M	g	M	g	M
Deoxygenated water	150.0		150.0		150.0		150.0	
AMA-80	1.01	0.019	1.00	0.019	1.00	0.019	1.00	0.019
Acrylic acid	0.45	0.042	0.88	0.081	–	–	0.45	0.042
Perdeuterated styrene	1.02	0.061	1.13	0.067	–	–		
Perdeuterated acrylic acid	–		–		0.42	0.037		
Styrene	–		–		1.12	0.072	1.00	0.065
Potassium persulfate	0.063	0.0015	0.069	0.0017	0.07	0.0017	0.067	0.0016

stabilized (AMA80) polystyrene latex (Fig. 3). At high pH the electrosterically stabilized polystyrene latex showed no turbidity even at the highest [KCl] (2.5 M); consequently no CCC could be determined for it at this pH. This pH dependence demonstrated quite clearly that the latexes produced by the batch polymerization described above were electrosterically stabilized.

2.2. SANS experiments

Aliquots of latexes A, B and C were added to blends of 7 mM solutions of sodium phosphate in H_2O and D_2O to give samples of equal electrolyte concentration over a range of contrast variations at pH = 8.5 (at which a significant degree of ionization of the carboxylate groups would be expected [2]). Electrolyte at this pH and similar concentration has been shown to expand the hairy layer slightly, presumably because the higher ionic strength facilitates ionization of the weak acid groups. Complete ionization of the carboxylate groups [2] requires pH ~ 10; however, at pH 10 the hairy layer would probably be so hydrated as to be indistinguishable from the continuous phase. Similarly, 0.03 M hydrochloric acid was used for pH 2 samples, which would be expected to be completely deionized.

SANS experiments were performed on the NG7 30 m SANS instrument at the NIST Center for Neutron Research in Gaithersburg, MD [26]. Neutrons of wavelength $\lambda = 1$ nm with a distribution of $\Delta\lambda/\lambda = 11\%$ were incident on samples contained within quartz cells. A sample-to-detector distance of 13.2 m was used to acquire data over a Q range of $0.0337 < Q < 0.33$ nm^{-1}, where Q is the magnitude of the scattering vector, defined below. Sample scattering was corrected for background and empty cell scattering, and individual detector pixel sensitivity. The corrected data sets were circularly averaged and placed on an absolute scale using standard samples and software supplied by NIST [27].

The structure of the model individual particle consisted of an impenetrable polystyrene spherical core and a concentric surface layer of poly(styrene-acrylic acid) into which solvent could freely penetrate. The SANS intensity $I(Q)$ from such an ensemble of particles in solution for a given value of the momentum transfer vector $Q = 4\pi/\lambda \sin(\theta/2)$ is given by Ref. [28]:

$$I(Q) \approx nP(Q)S(Q) \quad (1)$$

where θ is the scattering angle, λ is the neutron wavelength, n is the number density of particles, $P(Q)$ is the intraparticle form factor and $S(Q)$ is the interparticle structure factor. For dilute samples where interparticle interactions are negligible, the structure factor approaches unity ($S(Q) \approx 1$), permitting a simplified expression for the scattered intensity

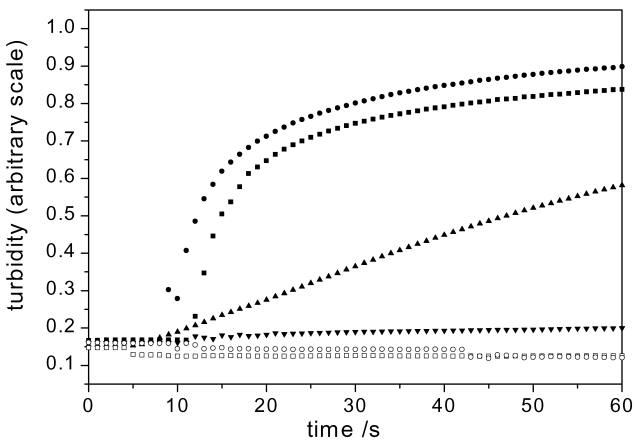

Fig. 2. pH and [electrolyte] dependence of turbidity as function of time for electrosterically stabilized polystyrene latex. Solid markers: pH 2; [KCl]/M: ■ 0.8; ● 0.6; ▲ 0.4; ▼ 0.2; open markers: pH 11; [KCl]/M: □ 0.8; ○ 2.5.

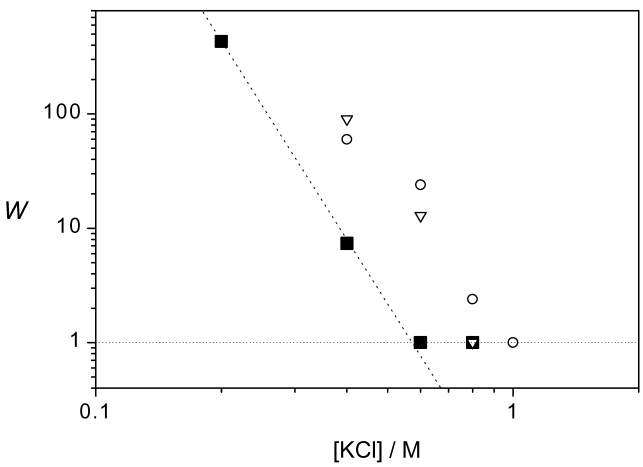

Fig. 3. CCCs measured by turbidimetry. ■ poly(styrene-co-AA), pH 2; ○ polystyrene/AMA-80, pH 2; ▽ polystyrene/AMA-80, pH 11.

[28]:

$$I(Q) \approx nP(Q) \quad (2)$$

Model calculations were performed for a spherical particle with a core-shell structure form factor (i.e. the density being a step function) [29], which is averaged over a Schulz distribution of sphere radii. The Schulz distribution is characterized by a polydispersity $p = \sigma_R/R$, where σ_R^2 is the variance of the distribution and R is the number-averaged particle radius. The shell thickness is considered to be a constant ratio of the core radius. Model fitting was accomplished using a standard non-linear least squares fitting routine.

3. Results and discussion

Six sets of data were acquired for three latexes at high and low pH (8.5 and 2, respectively). Figs. 4 and 5 are typical of the scattering from latexes A and B (perdeuterated styrene/protonated AA). The obvious features are the decrease in intensity and the change in shape of the scattering curves as the contrast-match point is approached. Fig. 6 is typical of the scattering arising from latex C (perdeuterated AA/protonated styrene). This is a little more complex as the contrast-match point is in the middle of the range of continuous-phase SLDs. However, it is clear that the curves change shape significantly with changing continuous-phase SLD and thus provide the variation required for reliable data fitting and parameterization thereby for latex C.

It can be seen in this work (Fig. 5) that near the contrast-match point the curves change shape dramatically. In fact at, or near, the contrast match point for latexes A and B it is clear that the scattering curve is almost the 'inverse' of the scattering curves at higher core/continuous-phase contrast in that the minima in the contrast-matched scattering curves are seen at approximately the same scattering angle as the maxima of the scattering curves at higher core/continuous-phase contrast. This confirms that the continuous-phase SLD is very close to the core SLD in these experiments and is a 'model-independent' means of estimating the core SLD. Allowing 1% for weighing and material transfer errors due to the small aliquots of stock latex (~30–50 mg), H_2O and D_2O (0–300 mg) used to prepare the samples, the SLDs of latexes A and B determined by this method were both $6.25 \pm 0.06 \times 10^{10}\ \mathrm{cm}^{-2}$. It is then a trivial matter to calculate the proportion of AA incorporated into the perdeuterated polystyrene latexes as 3.5 ± 1.5%.

For latex C there were no data close enough to the match point to estimate the core SLD by this means (and insufficient beam time for the extra experiments required to obtain such data).

Under appropriate experimental conditions (i.e. dilute enough to avoid significant multiple scattering and structure factor effects) and in the Guinier region (i.e. $Q < 1/R$ and the approximations invoked by Guinier to derive an analytic

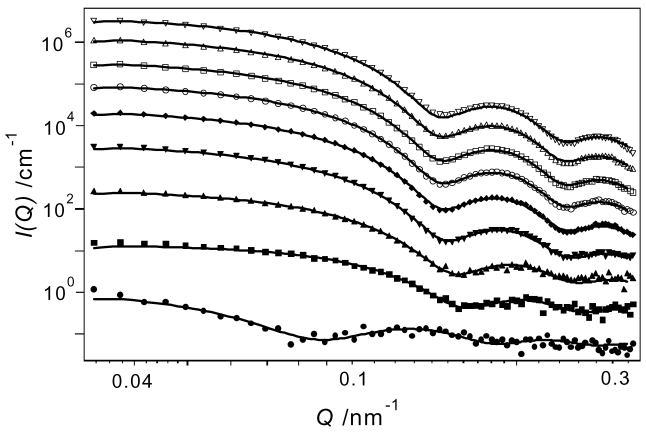

Fig. 4. $I(Q)$ vs Q, Latex A, deuterated core, pH 2. SLDs (× scaling): ●: 5.89 (× 1); ■: 5.65 (× 5); ▲: 5.47 (× 20); ▼: 4.85 (× 30); ◆: 3.93 (× 50); ○: 2.98 (× 100); □: 2.06 (× 200); △: 1.15 (× 500); ▽: 0.33 (× 1000).

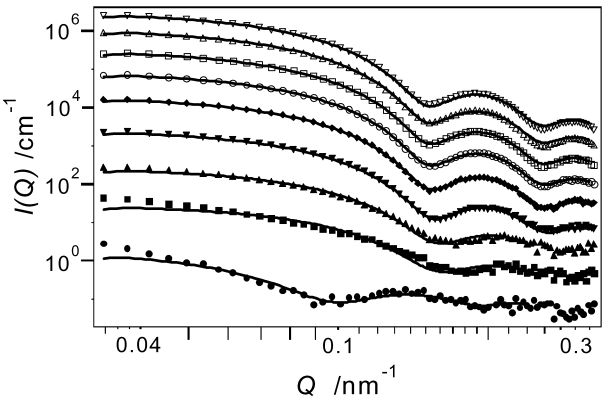

Fig. 5. $I(Q)$ vs Q, Latex B, deuterated core, pH 2. SLDs (× scaling): ●: 5.96 (× 1); ■: 5.75 (× 5); ▲: 5.56 (× 20); ▼: 4.95 (× 30); ◆: 4.04 (× 50); ○: 3.11 (× 100); □: 2.23 (× 200); △: 1.28 (× 500); ▽: 0.44 (× 1000).

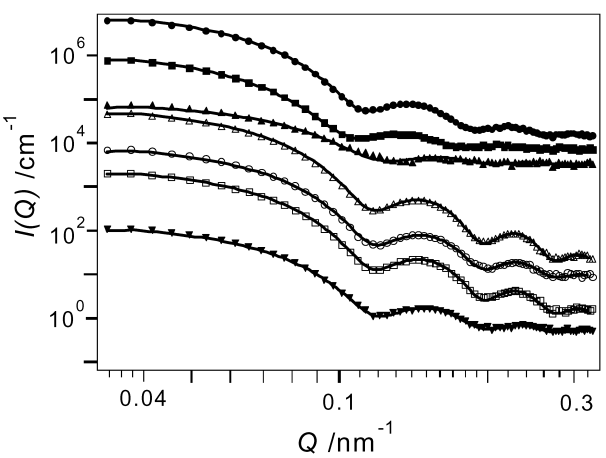

Fig. 6. $I(Q)$ vs Q, Latex C, deuterated shell, pH 8.5. SLDs (× scaling): ●: 0.06 (× 15,000); ■: 1.06 (× 10,000); ▲: 2.21 (× 6,000); ▼: 2.88 (× 1, ○: 20 (× 1); □: 3 (× 1), △: 40 (× 1).

solution are deemed to be acceptable), one has [28]:

$$I(Q) \propto (\rho_{\text{sample}} - \rho_{\text{contphase}})^2 \quad (3)$$

where ρ_{sample} is the sample SLD and $\rho_{\text{contphase}}$ is the continuous-phase SLD. Thus, for a dispersion of homogeneous particles a plot of $\sqrt{I(Q)}$ vs $\rho_{\text{contphase}}$ is linear and has an intercept (with the $\rho_{\text{contphase}}$ axis) that is equal to the SLD of the sample (Fig. 7). In this work there are several complications to consider. Firstly, the particles are not homogeneous. However, noting that $I(Q) \propto \Delta\rho^2$, it can be seen in Fig. 7 that, except at the lower continuous-phase/core contrasts, scattering from the shell is negligible, and thus at the higher contrasts the latexes appear almost homogeneous to a neutron (at least for latexes A and B). Secondly the SLD of the shell varies with the SLD of the continuous-phase (mainly because of the hydration of the shell but also due to proton/deuteron exchange between the pAA carboxylate and the continuous-phase). Consequently the SLD of the sample is also a weak function of the continuous-phase SLD. Once again, except at the lower continuous-phase/core contrasts, scattering from the shell is negligible and a linear fit to the rest of the data is valid. Thirdly, the condition that $Q < 1/R$ implies that this relation is truly valid for latexes A and B (radii ~30 nm) only when $Q < 0.033\ \text{nm}^{-1}$ and for latex C (radii about 40 nm) when $Q < 0.025\ \text{nm}^{-1}$. In this work, the smallest reliable Q is $0.0337\ \text{nm}^{-1}$, which is outside the Guinier region. Nevertheless, it can be seen (Fig. 7) that $\sqrt{I(Q)}$ remains proportional to the continuous-phase SLD. Thus a linear fit to $\sqrt{I(Q)}$ at $Q = 0.0337\ \text{nm}^{-1}$ yields a second, model-independent, estimate of the core SLDs, at least for latexes A and B. Once again, allowing 1% for weighing and material transfer errors, $\text{SLD}_{\text{latex A}} = 6.23 \pm 0.06 \times 10^{10}\ \text{cm}^{-2}$ and $\text{SLD}_{\text{latex B}} = 6.25 \pm 0.06 \times 10^{10}\ \text{cm}^{-2}$. In the case of latex C, scattering from the shell is significant over much of the range of continuous-phase SLDs and thus the homogeneous assumption does not hold (Fig. 7). Hence, a Guinier fit is inapplicable here.

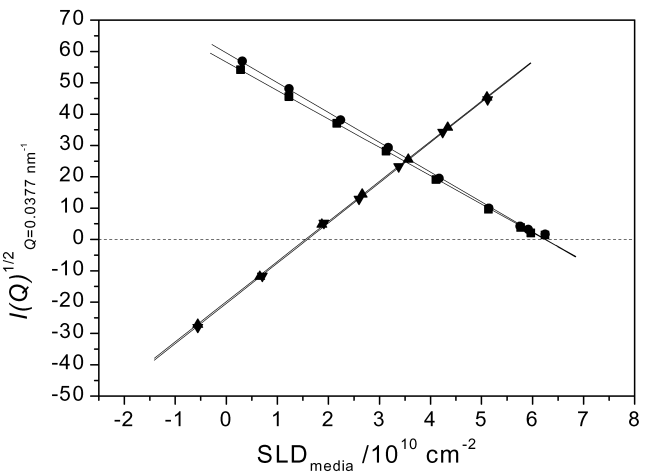

Fig. 7. $\sqrt{I(Q)}$ vs SLD media. ■ deuterated core, pH 8.5; ● deuterated core pH 2; ▲ deuterated shell, pH 8.5; ▼ deuterated shell, pH 2.

3.1. Model fitting

Data were least-squares fitted to a standard core/shell model 'smearpolycoreshellratio' provided by NIST.

It should be emphasized that models for SANS employ many parameters, in this case eight—solids content, core radius, shell thickness, polydispersity, core SLD, shell SLD, continuous-phase SLD and background. However, many of these can be determined, or at least narrowly constrained, by independent means. Thus, solids content of samples may be measured gravimetrically, core radius and polydispersity estimated from TEM (Fig. 1, Table 2), core SLD estimated from $\sqrt{I(Q)}$ as a function of continuous-phase SLD (Fig. 7), continuous-phase SLD calculated from weighed inputs and background neutron flux taken from the high-Q region of the SANS data (Figs. 5 and 6), leaving only the shell SLD and thickness as free variables.

Continuous-phase SLDs were allowed to float 1% about the values calculated from weighed inputs to allow for weighing uncertainties (as described above) and likely isotopic impurity of the D_2O, which is extremely hygroscopic and which exchanges with atmospheric H_2O during sample preparation and storage.

Unfortunately, gravimetry performed on the small quantities of material available was found to be unreliable and a less direct method had to be employed to determine solids content of the samples. For example, in Fig. 8 experiments 5–9 (noting that $I(Q) \propto \Delta\rho^2$), it is clear that the contribution to $I(Q)$ from the shell is negligible. As scattering from the core is proportional to solids content and also proportional to $\Delta\rho^2$, a reliable value for the solids content was obtained from these data. The accuracy of this method depends on the accuracy of the calculated continuous-phase SLDs (about 1% as described above); consequently in the data fitting the solids content was also allowed to float by a maximum of 1%. Ultimately, best fits were obtained with a variation from the calculated values much smaller than 1% for most samples.

3.2. Application of contrast variation

For the perdeuterated core latexes, shell thickness and SLD were determined from best fits to the SANS data obtained at or near the contrast match points (e.g. Expts 1, 2 and 3 in Fig. 8,). Experiments 5–7 are clearly insensitive to scattering from the shell and so are useful for characterizing the core. Thus the core radii and polydispersity were refined from the TEM estimates by fitting to the SANS data

Table 2
Latex core diameters (nm) determined by TEM and SANS

	Latex A	Latex B	Latex C	Undeuterated
SANS	63.6	60.6	80.8	n/a
TEM	61	58	80	70

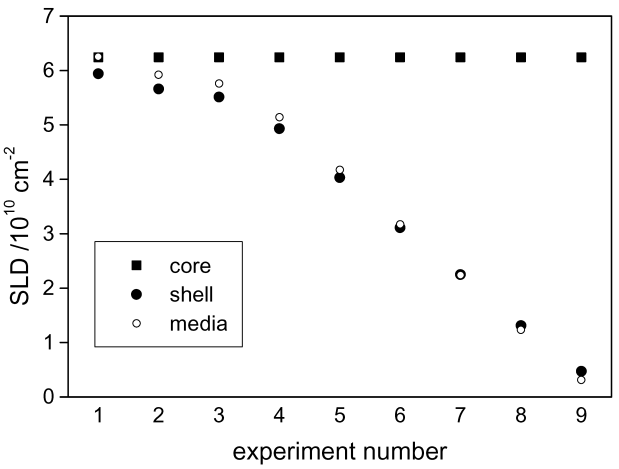

Fig. 8. Typical SLDs for deuterated core experiments, Latex B, pH 2.

corresponding to experiments such as experiment 7 in Fig. 8.

Similarly, for the perdeuterated shell latexes the core radii and polydispersity were refined from the TEM estimates by fitting to the SANS data corresponding to experiments such as experiment 7 in Fig. 9. Shell thickness and SLD were obtained from SANS data corresponding to experiments such as experiment 2 in Fig. 9.

From the shell SLDs it is a trivial matter to calculate the degree of hydration, taking into account the specific volume of pAA in aqueous solution, (0.73 $cm^3\ g^{-1}$ at 20–22°C) [30], continuous-phase SLD and exchange of deuterium on the carboxylates.

All fifty datasets were then modelled with the parameters determined as described above and listed in Tables 3 and 4. Typical fits are shown in Figs. 4–6.

It is clear (Figs. 8 and 9) that there is significant scattering from the shell for at least the three lowest contrasts in each set of data. Furthermore, the minima of the four lowest contrast curves in Figs. 4 and 5 clearly shift in a fashion that can only be ascribed to scattering from the shell. Thus the refinement of the parameters to achieve a best fit to

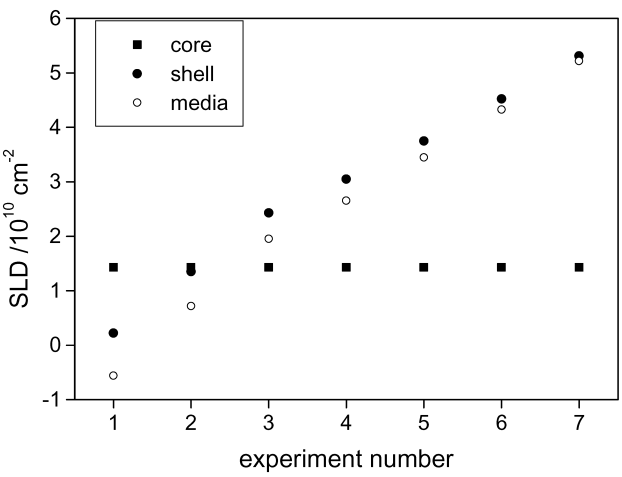

Fig. 9. Typical SLDs for deuterated shell experiments, Latex C, pH 2.

Table 3
Effect of pH on latex characteristics estimated from fits to SANS data

Latex	pH	Shell thickness (nm)	Shell hydration (Volume % H_2O)
A	2	3.5	89 ± 2
A	8.5	5.0	96 ± 2
B	2	4.3	91 ± 2
B	8.5	7.0	96 ± 2
C	2	4.4	87 ± 2
C	8.5	6.0	92 ± 2

four sets of data for each latex at both high and low pH should be quite reliable.

4. Inferences and conclusions

Before any conclusions may be drawn regarding the perdeuterated latexes it is necessary to consider what effects perdeuteration may have on the formation of these latexes. Perdeuteration is known to increase the propagation rate coefficient k_p by less than 50% [31]. This in turn affects reactivity ratios so that the proportion of a given monomer in a copolymer increases upon perdeuteration. Consequently, in a perdeuterated styrene/protonated AA latex, more styrene would be expected to be incorporated into the 'hairs' than in an otherwise similar protonated styrene/perdeuterated AA latex, resulting in shorter 'hairs' as the critical DOP for entry decreases with increasing styrene. This is consistent with the observation that latex A has a slightly thinner shell than latex C (Table 3), though clearly the effect on the hairy layer is small.

The first conclusions to be drawn from the experiments described herein are in accord with what one might expect from the known chemistry of pAA. These are that the hairy layer is highly hydrated and that the degree of hydration is pH-dependent, being approximately 94 ± 2% at low pH and 89 ± 2% at high pH. This high degree of hydration is consistent with the findings of Fritz et al. [20], who used very different techniques to show that electrosteric stabilizers (poly(methacrylic acid) in their case) have relatively high hydrodynamic permeability.

The composition of the hairy layer (i.e. the proportion of styrene in the AA/styrene hairs) could not be determined from these experiments because, in the experiments that were sensitive to the hairy layer, styrene was 'matched out'.

Table 4
pH-independent parameters determined from best fit to model. Volume % solids is the total core volume as a percentage of the total sample volume

Parameter	Latex A	Latex B	Latex C
Volume % solids	0.81 ± 0.04	0.83 ± 0.06	0.54 ± 0.02
Polydispersity	0.05	0.04	0.02
Core SLD/10^{10} (cm^{-2})	6.27	6.24	1.43
Core radius (nm)	31.8	30.3	40.4

A sensitivity analysis demonstrated a very small dependence of the fitted degree of hydration on the assumed proportion of styrene incorporated into the hairy layer. From best fits to all the data the degree of hydration varied by only about 2% when the assumed proportion of styrene was varied from 0–30%.

Secondly, the amount of AA incorporated in the core of the particles is 3.5 ± 1.5% of the total core volume. This is comparable to literature values determined by titration and mass balance. Thus in the most similar latex preparation found in the literature for which such data are available, Slawinski et al. [32] found that 'buried' AA comprised about 1% of the core volume in a styrene/AA latex prepared at 80°C and pH 2.5 [32]. Similarly, Dos Santos, McKenna and Guillot [33] reported that 'buried' AA comprised about 2% of the core volume in a styrene/BA/AA emulsion prepared at 60°C and pH 2.2 [33].

Thirdly, the pAA/styrene layer grown under the conditions of these experiments was about 3.5–7 nm thick, depending on pH and initial [AA]. This is an interesting result as it allows for a crude estimate of the DOP of the entering species in a styrene/AA copolymerization and supports speculation regarding the entry mechanism as follows. The most simplistic treatment would be to assume that the length of the hairs would be the critical DOP at which an aqueous-phase oligomer, of composition SO_4^--poly(AA)-*random*-polystyrene, becomes surface-active, analogous to what is seen in electrostatically stabilized systems. Now, the DOP of the entering species may be estimated from the shell thickness from the relation:

$$n = 6s^2/C_\infty l^2 \tag{4}$$

where n is the DOP, s is the radius of gyration of the polymer coil (i.e. 3/5 of the hydrodynamic radius and therefore 3/10 of the shell thickness), C_∞ is the characteristic ratio (assigned a value of 6.7, this being a copolymer of hydrophilic and hydrophobic monomers, for which C_∞ values range from 3–8 in a range of solvents) and l is the carbon–carbon bond length. This gives the DOP as about 40 for latex A and 70 for latex B (which had double the $[AA]_{aq}$ of latex A). If, as seems likely, the hairs are not simply random coils but are packed tightly onto the particle surface, the actual DOP would be somewhat less than that calculated in this way.

These values, for a system with a synthesis temperature of 90 °C, can be compared to the DOPs of the oligomers found in the aqueous-phase by Wang and Poehlein [34] at 50 °C: ~7 and ~15 for styrene/acrylic acid ratios from 9:1 to 6:4. Although the trend with $[AA]_{aq}$ is the same, the present values are greater. This difference may possibly be due to the significant temperature difference.

Van der Maarel et al. [35] measured corona thickness in polyelectrolyte diblock copolymer micelles with an acrylic acid block of DOP 85. They reported shell thickness from about 10–20 nm depending on degree of neutralization and electrolyte concentration and concluded that the hairs had adopted a rod-like configuration. As the hairs in the particles in the present study incorporate styrene, a rod-like configuration would be tempered by the hydrophobicity of the styrene units (and the presumably lower packing density of the hairs on a relatively large particle compared to that on a micelle) and hence the smaller shell thickness measured herein is consistent with a hydrophilic coil of similar DOP.

The fourth point is the dependence of shell composition and thickness on $[AA]_{aq}$. One can crudely estimate the effect of $[AA]_{aq}$ on copolymer composition from published reactivity ratios [30] and aqueous-phase monomer concentrations. There is considerable scatter in the literature reactivity ratios [30], but the mean is about $r_1 \sim r_2 \sim 0.2$; the composition of the 'hair' can then be calculated from values of the aqueous-phase concentrations of the two monomers, using the conventional Mayo terminal model. This simple approach gives the 'hair' composition as about 13% styrene for $[AA]_{aq} = 0.2$ M and $[\text{styrene}]_{aq} = 7 \times 10^{-3}$ M (its water solubility at 90 °C as estimated from a fit of the van't Hoff equation to published water-solubility data over the range 7–65 °C [36]), and about half that for $[AA]_{aq} = 0.4$ M. This accords with aqueous-phase copolymer compositions determined experimentally by Wang and Poehlein [34]. Furthermore, as is argued below, the effect of $[AA]_{aq}$ on shell thickness can be used to discriminate between entry models. Now, this calculation is very simplistic. Clearly, the aqueous-phase monomer concentrations change during the course of the polymerization, and consequently so does the composition of the copolymer species entering the particles. Moreover, several poorly quantified factors affect the composition. Firstly, it is well known that k_p for AA is strongly dependent on aqueous-phase concentration and on pH [4,5]. Secondly, the isotope effect described above will also have a small effect in experiments where deuterated monomers are used. However, as the latexes were grown at low [AA] and low pH where the AA is fully protonated, as a first approximation it is probably indicative of the composition of the 'hairs'. The important inference is that under the conditions of the polymerization, the 'hairs' are expected to incorporate a significant proportion of styrene (although the SANS experiment would be insensitive to its presence). Theory is starting to become available [37] which in the future might enable thickness of electrosteric stabilizers to be calculated from composition.

4.1. Kinetically controlled entry model

The 'z-mer' model for entry [8], so successful in electrostatically stabilized systems, supposes that entry occurs if and only if the aqueous-phase oligomeric radical grows sufficiently (to a DOP z) to become surface-active. A possible starting point to extend this to electrosterically stabilized particles would be to assume that entry will occur

when two hydrophobic units form a diad in the aqueous-phase propagation process. If one assumes that entry is likely upon formation of a styrene diad and that the grafted 'hairs' are configured as random coils, then shell thickness will be proportional to $[AA]_{aq}$ as follows. The number of AA units added per styrene addition is proportional to $[AA]_{aq}$. Concurrently, the probability of an aqueous-phase oligomer with a styrenic radical endgroup adding a styrene monomer unit to form a styrene diad is inversely proportional to $[AA]_{aq}$. Thus the DOP of the entering species should increase with $[AA]_{aq}^2$. As can be seen from Eq. (4), the radius of gyration (and hence the shell thickness) is proportional to $\sqrt{DOP}$ and therefore the shell thickness would be proportional to $[AA]_{aq}$. Thus this model is clearly not applicable, as doubling $[AA]_{aq}$ resulted in an increase of shell thickness of only about 20% (Table 3).

4.2. Thermodynamically controlled entry model

Dong and Sundberg [38] have put forward a thermodynamic model for entry in copolymerization using lattice theory to estimate chemical potential for aquation for oligomers. Their model predicts critical degrees of polymerization ~ 10 for styrene/acrylic acid at 50 °C for copolymers containing 90% acrylic acid. This value is significantly less than that at 50 °C reported by Wang and Peohlein for the largest DOP of aqueous-phase oligomers [34], and much less than that implied here for 90 °C. Given that Dong and Sundberg suggest that the temperature dependence of the input parameters to the model is small, their model does not seem to be in accord with the present data.

We put forward here a supposition for the basis of an alternative model, which supposes that addition of AA units at pH 3 has little or no effect on the free energy of hydration of the growing aqueous-phase oligomeric radicals and that the hydrophobicity of the growing aqueous-phase oligomeric radical depends primarily on the total number of styrene units incorporated. Doubling the $[AA]_{aq}$ would then be expected to nearly double the DOP at which the growing aqueous-phase oligomeric radical incorporates enough styrene to attain sufficient hydrophobicity for its radical center to irreversibly enter a particle. This is consistent with the calculated increase (by a factor of 1.7) in the DOP of the entering species of latex B compared to those of latex A as determined from the shell thickness in each case.

In conclusion, the observed dependence of hairy layer (shell) thickness on the initial amount of acrylic acid suggests that the critical DOP for entry (and therefore covalently grafted) electrosteric stabilizer is thermodynamically (not kinetically) controlled.

Acknowledgements

The support of a Large Grant from the Australian Research Council is gratefully acknowledged, as is the US National Institute of Standards and Technology. The Key Centre for Polymer Colloids is established and supported under the Australian Research Council's Research Centres Program.

References

[1] Gilbert RG. Emulsion polymerization: a mechanistic approach. London: Academic Press; 1995.
[2] Bassett DR, Hoy KL. In: Fitch RM, editor. Polymer colloids II. New York: Plenum Press; 1980. p. 1.
[3] Napper DH. Polymeric stabilization of colloidal dispersions. London: Academic Press; 1983.
[4] Kuchta F-D, Van Herk AM, German AL. Macromolecules 2000;33:3641.
[5] Lacik I, Beuermann S, Buback M. Macromolecules 2001;34:6224.
[6] Ganachaud F, Balic R, Monteiro MJ, Gilbert RG. Macromolecules 2000;33:8589.
[7] Vorwerg L, Gilbert G. Macromolecules 2000;33:6693.
[8] Maxwell IA, Morrison BR, Napper DH, Gilbert RG. Macromolecules 1991;24:1629.
[9] Coen E, Lyons RA, Gilbert RG. Macromolecules 1996;29:5128.
[10] Gilbert RG. In: Asua JM, editor. Polymeric dispersions. Principles and applications. Dordrecht: Kluwer Academic; 1997. p. 1.
[11] van Berkel KY, Russell GT, Gilbert RG. Macromolecules 2003;36:3921.
[12] De Bruyn H, Miller CM, Bassett DR, Gilbert RG. Macromolecules 2002;35:8371.
[13] Morrison BR, Maxwell IA, Gilbert RG, Napper DH. In: Daniels ES, Sudol ED, El-Aasser M, editors. Polymer latexes—preparation, characterization and applications. ACS symposium series, Washington, DC: American Chemical Society; 1992. p. 28.
[14] Morrison BR, Casey BS, Lacík I, Leslie GL, Sangster DF, Gilbert RG, Napper DH. J Polym Sci A: Polym Chem 1994;32:631.
[15] Poehlein G. Macromol Symp 1995;92:179.
[16] Bassett DR, Derderian EJ, Johnston JE, MacRury TB. In: Bassett DR, Hamielec AE, editors. Emulsion polymers and emulsion polymerization. ACS symposium series No. 165, Washington, DC: American Chemical Society; 1981. p. 263.
[17] Guo X, Weiss A, Ballauff M. Macromolecules 1999;32:6043.
[18] Charmot D, D'Allest JF, Dobler F. Polymer 1996;37:5237.
[19] van den Hul HJ, Vanderhoff JW. Br Polym J 1970;2:121.
[20] Fritz G, Schadler V, Willenbacher N, Wagner NJ. Langmuir 2002;18:6381.
[21] Bassett DR. In: Poehlein GW, Ottewill RH, Goodwin JW, editors. Science and technology of polymer colloids. NATO ASI series, Amsterdam: Martinus Nijhoff; 1983. p. 220.
[22] Dingenouts N, Pulina T, Ballauff M. Macromolecules 1994;27:6133.
[23] Ballauff M, Bolze J, Dingenouts N, Hickl P, Potschke D. Macromol Chem Phys 1996;197:3043.
[24] Ottewill RH. Pure Appl Chem 1992;64:1697.
[25] Overbeek JTG. Adv Colloid Interface Sci 1982;16:17.
[26] Glinka CJ, Barker JG, Hammouda B, Krueger S, Moyer JJ, Orts WJ. Appl Crystallogr 1998;31:430.
[27] NIST, SANS Data Reduction Software.
[28] Guinier A, Fournet G. Small-angle scattering of X-rays. New York: Wiley; 1955.
[29] Hayter JB. In: Degiorgio V, Corti M, editors. Physics of amphiphiles—micelles, vesicles, and microemulsions. New York: Elsevier Science Publishing Company; 1985. p. 59.
[30] Brandrup J, Immergut EH, Grulke EA, editors. Polymer handbook. New York: Wiley; 1999.

[31] Olaj OF, Schnöll-Bitai I. Makromol Chem, Rapid Commun 1990;11: 459.
[32] Slawinski M, Schellekens MAJ, Meuldijk J, Van Herk AM, German AL. J Appl Polym Sci 2000;76:1186.
[33] Santos AM, McKenna TF, Guillot J. J Appl Polym Sci 1997;65:2343.
[34] Wang S-T, Poehlein GW. J Appl Polym Sci 1993;50:2173.
[35] van der Maarel JRC, Groenwegen W, Egelhaaf SU, Lapp A. Langmuir 2000;16:7510.
[36] Shiu W-Y, Ma K-C. J Phys Chem Ref Data 2000;29:41.
[37] Borisov OV, Leermakers FAM, Fleer GJ, Zhulina EB. J Chem Phys 2001;114:7700.
[38] Dong Y, Sundberg DC. Macromolecules 2002;35:8185.